Hindawi
Journal of Advanced Transportation
Volume 2018, Article ID 5876104, 8 pages
https://doi.org/10.1155/2018/5876104

Research Article

Modeling the Effects of Bus Stops on Bicycle Traffic Flow by Cellular Automata

Zhaoguo Huang, [1,2,3,4] **Xiucheng Guo**, [1,3,4] **Chunbo Zhang**, [1,3,4] **and Hongying Zhang** [2]

[1] *Jiangsu Key Laboratory of Urban ITS, Southeast University, China*
[2] *School of Civil Engineering, Lanzhou University of Technology, China*
[3] *Jiangsu Province Collaborative Innovation Centre of Modern Urban Traffic Technologies, Southeast University, China*
[4] *School of Transportation, Southeast University, China*

Correspondence should be addressed to Xiucheng Guo; seuguo@163.com

Received 28 February 2018; Revised 5 July 2018; Accepted 6 August 2018; Published 2 September 2018

Academic Editor: Antonio Comi

Since currently huge traffic demands for public bus and bicycles exist in the majority of cities of China, it is highly likely that the bus stop has undeniable impacts on the bicycle flow that is close to the bus stop. In this paper, we proposed the test in several bicycle paths beside bus stops in Nanjing and aimed at exploring the specific effects of bus stop on the bicycle flow nearby. We assumed there were two such effects: space restriction and pedestrian conflicts. Further, we built up a cellular automation (CA) model to study the feature of these effects and find out not only the outcome of these two effects, but also the inner correlation between them.

1. Introduction

The bicycle travel for utilitarian purpose plays a significant role in the large cities of China. Abundant city roads are equipped with facility for thousands of bicycle user for the purposes of commuting or relaxing. However, the design of bicycle facility on the road [1], which is not the focus in designing a road, has several problems that cause bicycle traffic flow hardly to run smoothly, such as the red-light running [2, 3] and bicycle conflicts with other road users [4]. One of the problems on the bicycle path is the effect of bus stop, as showed in Figure 1, on bicycle traffic flow.

In this study, we assumed the bus stop has two main kinds of effects on bicycle traffic flow: (1) pedestrians who cross the bicycle path: in order to travel between the bus stops and the main pedestrian street, bus users have to cross the bicycle path and thus cause delay and potential dangers on the bicycle; (2) some bus stops, specifically harbor-shaped bus stops, demanding land space from bicycle path reduce the width of bicycle path and influence the bicycle flow performance.

In past several decades, traffic designers, planners, and scholars have paid much attention on the effects of bus stop on traffic flow. One prominent achievement is a set of guidelines for applying in designing and locating bus stop. The guidelines concluded the factors needed to consider when designing the l bus stop and also provided information about trade-offs among various bus stop treatments [5]. Koshy and Arasan studied the impacts of bus stops on the speed of vehicles by applying the microscopic traffic simulation model [6]. Moura et al. analysed optimal bus stop location using a sequentially applied two-stage model. The results obtained from the proposed model showed important differences in the commercial speed of the buses depending on the final location of the stop [7]. Zhao et al. analysed the capacity drop caused by the combination effects of signalised intersections and bus stops [8, 9]. Fitzpatrick and Nowlin investigated the effects of bus stop design on suburban arterial operations [10]. Nevertheless, only a few researches related to the impacts of bus stop on bicycle traffic flow. Zhang et al. analysed the influences of various types of bus stops on traffic operation of bicycles, vehicles, and buses. Four types of stops were considered according to the geometric feature and lane arrangement. The results showed that type 3 and type 4 stop had the least impact on bicycle speed [11]. Ranasinghe et al. investigated the saturation headway variation at signalised

Figure 1: Effects of bus stop on bicycle traffic flow.

intersection approaches with a downstream bus stop and bicycle lane. The results showed that buses significantly affect change mean saturation headway where bicycles do not [12]. Börjessonca et al. optimised the number of bus stops, and prices for car, bus, and cycling in the busiest inner city corridor in Stockholm. The authors found that, in the welfare optimum, the bus service only requires a small subsidy due to congestion in the bus lane, crowding in the buses, and extra boarding and alighting time per passenger [13].

Evaluation methods of Bicycle Level of Service (BLOS) have continually seen improvements and refinements. BLOS is set up based on the perceived hindrance to user by Botma, as a function of pedestrian and bicyclist volumes, path width, and speed [14]. According to 2010 Highway Capacity Manual (HCM), the disturbing events of bicycles have been divided into passing events and meeting event and occur when the bicycle encounters a bicycle in the same direction and opposing direction, respectively. HCM also define that the weighted sum of the number passing and meeting events is criterion used to determine level of service for bicycle paths [15]. Additionally, some research proposed several special cases of BLOS evaluation model as the extended application of the generalized BLOS evaluation model. Li et al. provided a special case of BLOS evaluation model conditioning on physically separated bicycle roadway [16, 17]. Minh et al. conducted a field video and found that the speed differences between passing and passed motorcycle were big [18].

Another area of intense research in the recent past is the application of cellular automation model (CA model) in simulation of traffic flow. This has been spurred by the increasing presence and utility of computer used for research. This tool is widely used to determine LOS measures for vehicle land and is expected to analyse the level of service for bike path construction. CA model has the advantage that it could operate computationally simply while providing rich behavior data for comparison to the empirical results and collection of the features of the bike flow. The basic process for CA model is the simulation rules' establishment and parametric calibration. Lin has summarized the previous studies and set up a set of detailed simulation definitions and update rules for CA model and validated the model with simulation experiments [19]. Gregory and Alex established CA model to analyse the service level of bicycle roadway and calibrated the model with data [20]. Zhao used the CA method to model the characteristics of bicycle passing events in mixed bicycle traffic on separated bicycle paths. The CA model was calibrated with the use of the field data to simulate the passing events in the mixed bicycle traffic. The results showed that the CA model could simulate the features of bicycle passing events well [21]. Luo et al. proposed a CA model to simulate the car and bicycle heterogeneous traffic on urban road. To capture the complex interactions between these two types of vehicles, a novel occupancy rule is adopted in the proposed model. Results indicated that the constant and fixed occupancy rule adopted in the previous studies might lead to overestimation of car flux in the heterogeneous traffic flows with different bicycle densities [22]. Xue et al. modeled the bicycle flow using an improved Burgers CA model and the results showed that the improved model could effectively simulate the bicycle flow [23].

Literature review results showed the bus stops have a significant negative impact on traffic operation, and this is particularly true for bicycle flows. When a bus stop installed on a bike lane, the bicycle operation may be hindered because of the heavy pedestrian activities at the bus stop, resulting in the disturbance of bicycle flow. As such, there is a need to include the effects of bus stops when modeling the bicycle traffic flow. With the development of simulation techniques, CA model provided us with an efficient and flexible way to capture the bicycle flow characteristics at the bus stop bike lane. Within the CA model, each bicycle and pedestrian can be set as one cell. The parameters for each cell, such as the acceleration of bicycle, can be also set in a flexible way. Consequently, the interactions between pedestrians and bicycles can be simulated accurately.

The objective of this study is to investigate the effects of bus stop on the bicycle traffic flow. A cellular automation (CA) model is developed for this goal. Accordingly, the remainder of this paper is organized as follows. The next section specifies the data collection. The CA model for modeling bicycle traffic flow is given in Section 3. Section 4 introduces the CA models results and discussion. Finally, conclusions are presented in Section 5.

2. Data Collection and Description

Data of bicycle traffic flow on exclusive bicycle path is collected for the later simulation work. Field studies were carried out on two sections of exclusive bicycle paths in the center of Nanjing city: West Beijing Road and Longpan Road. We selected the sections near Gulou Bus Stop on West Beijing Road, which is a conventional bus stop, and the section around a harbor-shaped bus stop, Gangzicun Bus Stop, on Longpan Road, to compare and analyse the effect of alternative bus stop on bicycle traffic flow. Both selected sections are generally 3.5 m wide, smooth bicycle path, while the section near the harbor-shaped bus stop on Longpan Road is 2.5 m wide.

Cyclists are typically students, recreational users, and commuters. The selected bicycle paths have exclusive use. However, on certain sections of paths beside the bus stops pedestrians were allowed through to the bus stop. To collect field data, traffic scenes on the bicycle path section were recorded with video cameras by placing cameras on the pedestrian streets along the selected bicycle paths as shown in Figure 2. One hour of video was recorded on Gulou Bus

FIGURE 2: Field data collection.

Stop, and one hour of video was recorded on Gangzicun Bus Stop. The recording hours are enough for data collection due to the heavy bicycle traffic volume.

The recorded video tapes were reviewed in the laboratory for data reduction. The media software VideoStudio was used to estimate the bicycle/pedestrians flows, speeds, and conflicts. From the video we found that there exist two different treatments when cyclists meet conflicts with pedestrian. Some cyclists would reduce the bicycle speed and wait pedestrians crossing the path in prior, while others may maintain the speed through the conflict area before the pedestrians.

3. CA Model

The model implementation tool in this paper is MATLAB R2015a. In this paper, we simulated mixed bicycle flow and pedestrian flow with a multilane CA model, which includes three parts: CA model definition, updating rules, and simulation rules.

3.1. CA Model Definition

3.1.1. Cell Size. The CA model simulates bicycle roadway in unit of the cell, which represents a discrete specific section of the roadway. Cell size largely depends on the traffic density on the roadway and bicycle's physical size. During the simulation, each cell has only two states: occupied or not. We can refer to other research's definition on cell size to decide this index. Gregory Gould set 7 feet as the length of a bicycle cell, while both Zhang and Liu adopted 2 meters as the length of a bicycle cell.

Considering the impact of acceleration limits is 1.8m/s^2 (this will be discussed later) and bicycles' physical size, we set 2m as the length of a bicycle cell and choose 0.5m as the width of a bicycle cell.

3.1.2. Dimension. We have two dimensions set in our simulation. The x dimension represents the direction in which bicycle flow travels and the y dimension shows the lateral distance, which has boundaries as shown in Figure 3. The boundaries should be corresponded with the number of bicycle lanes.

In time t, the current position of bicycle n is $x_n(t)$ and y (t), and $d_n^1(t)$, $d_n^2(t)$, and $d_n^4(t)$, respectively, represent the forward space headways between current cell of the

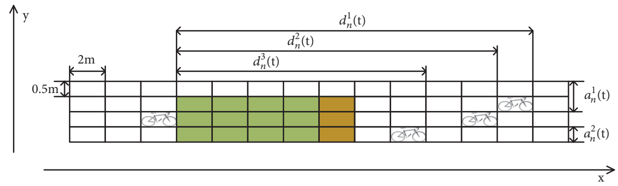

FIGURE 3: Illustration of the schematic diagram of cells on bicycle roadways.

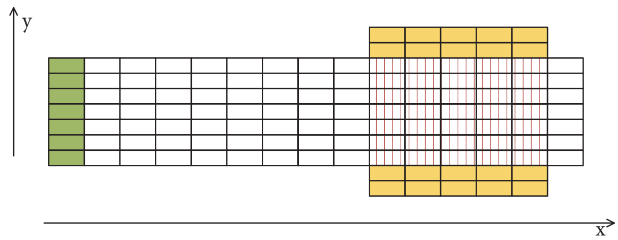

FIGURE 4: Illustration of modeling scene for conventional bus stop.

bicycle n and the nonoccupied cell in the left front, straight front, and right front side.

3.1.3. Modeling Bicycle Size. We set two modeling scenes, one for a bicycle path near the harbor-shaped bus stop and another for a bicycle path near the conventional bus stop.

The model for the bicycle path with the conventional bus stop is shown in Figure 4.

The modeled bicycle path is a matrix consisting of 7×80 cells, where the width of path valued 3.5m is as wide as seven cells and the length of path to test is set as long as eighty cells (160m), and the bus stop is located beside 51 to 55 cells in x dimension. The yellow area in Figures 4 and 5 represents the area to generate pedestrian flow to cross the path and cause conflicts on cyclists.

The model for the bicycle path with the harbor-shaped bus stop changes the location of bus stop compared with the path with conventional bus stop, whose bus stop occupies a few area from bicycle path and thus reduces the width of path to five cells (2.5m). The model is illustrated in Figures 4 and 5.

3.1.4. Bicycle's Speed. Bicycle's speed includes lateral speed and forward speed. Lateral speed is perpendicular to the street that occurs when bicycle changes lanes, and forward speed is parallel to the street. In this paper, v stands for the represented forward speed and v' for the lateral speed. We suppose that only the current lane and adjacent lanes are available for bicycle to run, which means the bicycle can only change at most one lane at a time unit.

In the CA model, we assume the simulated speeds of bicycles are discrete values: the forward speed could be 1, 2, 3, 4, and 5, where five (10m/s) is set as the fastest speed limit that bicycle could achieve. And bicycle's lateral speed could be -1, 0, and 1. The negative symbol represents the direction.

3.2. CA Model Updating Rules. In each step of simulation, bicycle's speed and position are updated according to the

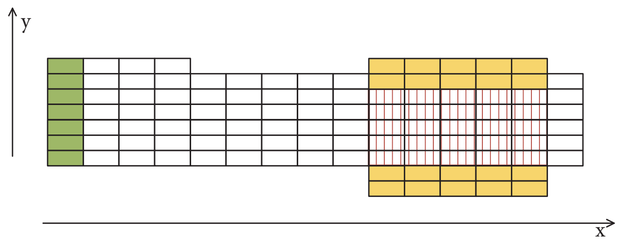

Figure 5: Illustration of modeling scene for harbor-shaped bus stop.

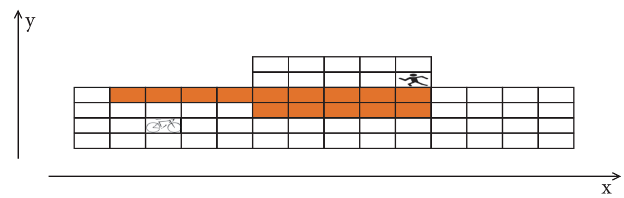

Figure 6: The influencing area of a pedestrian on bicycle flow.

basic movement schematic and the definition of speed above. The speed updating should be prior to position updating.

3.2.1. Updating Forward Speed. Normally bicycles tend to accelerate to its peak speed. However, the acceleration process is constrained from three restrictions:

(1) Bicycle Acceleration Ability. According to American Association of State Highway and Transportation Officials (AASHTO, 2001) [24], the maximum acceleration rate for an adult upright cyclist is 1.5 m/s^2. Though very few official documents have been made to define the acceleration of electric bicycle, it makes intuitive sense that the acceleration speed of electric bicycle is faster than the acceleration of conventional bicycle. As a result, we set overall bicycle's forward acceleration ability as $2m/s^2$ (1 cell). We assume the acceleration only takes place when the bicycle does not change lane.

(2) The Maximal Space That Allows Bicycle to Approach. The value of the maximal space d_{nmax} is selected based on the following schematic: If the bicycle is in the leftmost lane (or rightmost lane), we set the value d_{n1} (or d_{n3}) as 0 to prevent the bicycle out of the bicycle roadway. If $d_{n2} = \max\{d_{n1}, d_{n2}, d_{n3}\}$, then $d_{nmax} = d_{n2}$. If $d_{n2} \neq \max\{d_{n1}, d_{n2}, d_{n3}\}$ and $d_{n1} = d_{n3}$, then there is 50% chance that $d_{nmax} = d_{n1}$ and 50% chance that $d_{nmax} = d_{n3}$. Otherwise, $d_{nmax} = \max\{d_{n1}, d_{n3}\}$.

In addition, we set 6 as the safe distance that the bicycle does not need to change lane even when the forward space d_{n2} is the shortest distance.

(3) The Maximal Speed Limit, Which Is Defined as 5 in Section 3.1.4. The updating expression of a bicycle's forward speed is as follows: $v_n(t+1) = v_n(t) + 1$, if $d_{nmax} = d_{n2}.v_n(t+1) = \min\{v_n(t+1), d_{nmax}, v_{max}\}$.

3.2.2. Forward Speed Random Slowdowns. Although most bicycles try to run at its maximal speed for the utilization purpose, there are some uncertain factors disturbing bicycle flow that still may cause bicycle to slightly slow down. We define that the probability of a bicycle to randomly slow down is P_s, and when this happens, we have $v_n(t+1) = \max\{v_n(t+1) - 1, 1\}$.

Besides those uncertain impacts, the conflict with cross-street pedestrian also may cause the deceleration of bicycle. However, from the field study, not every bicycle will slow down when they meet conflict with pedestrian on the bicycle path; some of them simply maintain the forward speed and make pedestrian wait. We define the probability for a bicycle to slow down when it is influenced by a pedestrian as P_{sm} and the influence area showed in Figure 6.

The values of P_s and P_{sm} are calibrated later.

3.2.3. Updating Lateral Speed. From the former discussion, the lateral speed can only be -1, 0, and 1, respectively, representing the movement of changing to the left lane, continuing on the current land, and changing to the right lane. The movement of changing lane is dependent on the space headway: the bicycle will turn into the lane with the most forward space. The mechanism of this update is that bicycles tend to run on the lane with the longest space headway.

If $d_{nmax} = d_{n2}, v' = 0$; if $d_{nmax} = d_{n1}, v' = 1$; if $d_{nmax} = d_{n3}, v' = -1$.

3.2.4. Updating Position. The way to update position is merely by adding updated speed to the current position of the bicycle.

$$x_n(t+1) = x_n(t) + v_n(t+1) \tag{1}$$

$$y_n(t+1) = y_n(t) + v'_n(t+1) \tag{2}$$

3.3. Simulation Rules

3.3.1. Bicycle Initialization. The bicycle flow initialization consists of specific bicycle initialization with feature of density and speed distribution. The traffic volume and speed distribution could be gained from field survey. Then we have the density of bicycle flow based on the fundamental traffic flow theory: $k = Q/V$.

Figures 4 and 5 show the way to initial the bicycle flow. The green area is the potential cell to generate bicycle with probability P_{occ}, which represents the probability that a random cell in bicycle roadway is occupied. This value could be calculated as

$$P_{occ} = \frac{k}{maximal\ density} = \frac{k}{(1000/1.5) * 6} \tag{3}$$

According to the field study, the initial average speed is 6.525 m/s for the path with harbor-shaped bus stop, and the value for the path with conventional bus stop is 6.481 m/s. We assume the distribution of initial bicycle speed is normal distribution $s \sim N(\bar{v}, \sigma)$, and the value of σ is set as 0.6 with the field data. So the initial speed for a random bicycle in the model is int(s/2) cells.

3.3.2. Pedestrian Initialization. The yellow area and red area in Figures 4 and 5 show the potential cell to generate

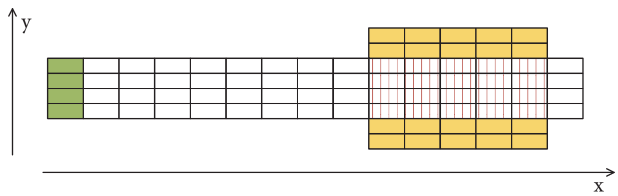

FIGURE 7: Illustration of initialization of bicycle and pedestrian travel.

pedestrians who are going to cross the bicycle roadway. The probability for a potential cell to generate a pedestrian in a time unit is based on the pedestrian rate.

Specific studies have found pedestrian walking speeds ranging from 1.253 m/s to 1.319 m/s. Considering this speed would be reduced when pedestrians cross the bicycle path, therefore, we set the pedestrian speed as a constant value of 1 m/s (2 cells).

3.3.3. Bicycles-Pedestrians Conflicts. For a normal pedestrian in a randomly selected marked cell, if there is at least one bicycle, regardless of the movement of changing lane, that could approach the cell in front of the pedestrian in a single time unit, or could approach the cell two steps before the pedestrian in a single time unit (orange area), the speed of pedestrian becomes 1. Otherwise, the speed of pedestrian becomes 2.

3.4. Traffic Features Detectors

3.4.1. Conflict Counter. Whenever there is a bicycle running into the conflicting area (orange area in Figure 7) of any pedestrian, we view it as an event of conflict. Finally we can obtain the conflicts number in each second and also the average conflicts number per second.

3.4.2. Influenced Speed Detector. This detector is used to record the bicycle traffic flow performance in the area beside the bus stop. We record the average speed of bicycles in the area of 50 to 65 in x dimension in each second and also the overall average speed of bicycle in this area across the whole modeling period.

3.5. Calibration of the CA Model. Most input value of model is selected as the same value of the field study, such as the initial speed of bicycle and pedestrian, the density of people and cyclists, and the geometric size of bicycle path. But the value of the probability of a bicycle to randomly slow down, P_s, and the probability of a bicycle to slow down when influenced by pedestrians, P_{sm}, remain unknown.

In this study, the least sum square was used to calibrate the value of P_s and P_{sm}. We set multiple scenarios for the values of P_s and P_{sm} varying from 0.1 to 1, respectively, with intervals of 0.1 for both. An iterative procedure was then followed to find out the optimum P_s and P_{sm}, which provide the least sum square of differences in simulated and observed average speed.

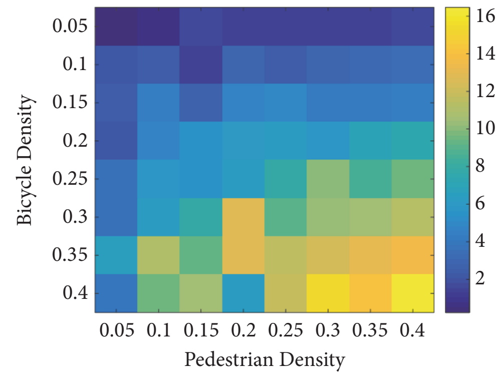

FIGURE 8: Average conflict numbers per second for path with harbor-shaped bus stop.

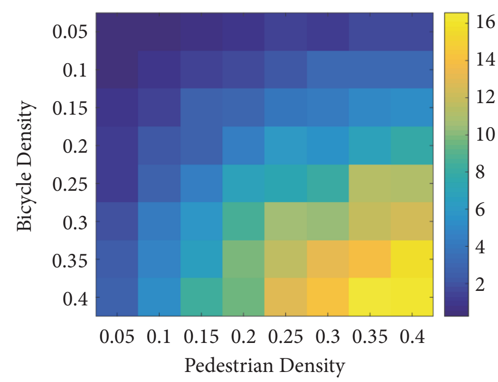

FIGURE 9: Average conflict numbers per second for path with conventional bus stop.

From Table 1, when values of both P_s and P_{sm} are 0.8, the minimal least sum square is obtained. This result is validated by corresponding to the field data where $P_{sm} = 0.75$.

4. Result Analyses and Discussion

We selected two indexes to indicate the performance of bicycle traffic flow: the average conflicting number per second and the average speed of influenced bicycle. Traffic flow performances under different conditions could reveal the effect of alternative bus stop condition on bicycle traffic flow.

4.1. Conflicts Number. The average conflict numbers per second for different scenes are showed in Figures 8 and 9, where blue areas indicate low conflict number while yellow indicates high conflict number with corresponding pedestrian density and bicycle density. (Lower conflict number is preferred.) Both pedestrian density and bicycle density vary from 0.025 veh/m^2 to 0.2 veh/m^2 with interval of 0.025 veh/m^2. The results show low conflicts frequency with low bicycle and pedestrian density, and the conflicts number increases with the incensement of bicycle and pedestrian density at both paths. This finding is reasonable because the potential of conflicts is low at free flow condition with low traffic density, while the possibility of conflicts increased at high traffic

Table 1: The least sum square (LSS) of speed differences with different probability of a bicycle to randomly slow down.

P_s	P_{sm} 0.1	0.2	0.3	0.4	0.5	0.6	0.7	0.8	0.9	1
0.1	11.020	10.776	9.985	10.690	9.124	8.456	7.893	7.717	7.603	7.085
0.2	10.027	9.953	9.899	7.930	8.531	6.600	6.531	6.659	5.045	4.192
0.3	9.157	8.683	7.987	8.217	5.958	6.017	4.855	5.478	2.868	3.425
0.4	8.270	7.318	6.485	5.824	4.722	3.875	4.155	3.036	4.089	2.418
0.5	7.123	6.142	5.962	4.985	4.770	2.519	2.227	1.727	1.855	0.579
0.6	6.015	5.616	4.844	3.718	2.655	2.112	3.129	1.857	0.831	0.165
0.7	5.146	4.813	2.370	1.890	1.577	1.018	0.468	0.291	0.196	0.092
0.8	3.281	2.381	1.308	0.440	0.681	0.504	0.107	0.016	0.048	0.290
0.9	0.577	0.730	0.080	0.030	0.129	0.442	1.025	1.265	1.388	2.426
1	2.167	2.889	2.108	2.569	3.108	3.649	3.753	4.582	4.581	4.762

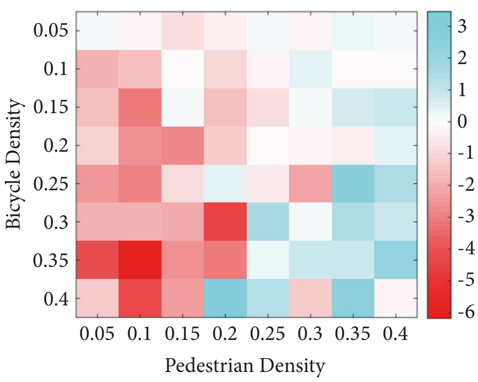

Figure 10: Difference of average conflict numbers per second between the scene with harbor-shaped bus stop and conventional bus stop.

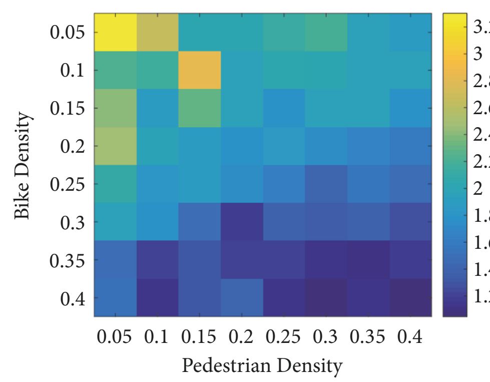

Figure 11: Average influenced bicycle speed for path with harbor-shaped bus stop.

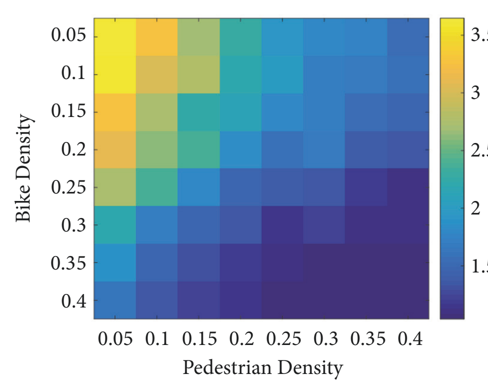

Figure 12: Average influenced bicycle speed for path with conventional bus stop.

density condition due to the increasing interactions between bicycles and pedestrians [3, 7]. It was also found that conflicts frequency at harbor-shaped bus stop area is higher than that at conventional bus stop area for the same bicycle and pedestrian density. This result indicates that the harbor-shaped bus stop has more impact of bicycle traffic flow in reflection of increased conflicts, which can be explained as harbor-shaped bus stop could reduce the width of bicycle path.

In Figure 10, red area indicates that the average conflict number per second in the scene with the harbor-shaped bus stop is larger than that in the scene with the conventional bus stop, and blue area indicates the counter relationship. It can be concluded that pedestrian density has little influence when bicycle density is at low level. When bicycle density is high, pedestrian density causes significant change on the number of conflicts, as harbor-shaped bus stop has more conflicts when pedestrian density is low, but conventional bus stop has more conflicts when pedestrian density is high. This result is consistent with previous studies of [1, 3] which showed various impacts of bicycle and pedestrian density on conflicts frequency.

4.2. Speed Performance of Influenced Bicycles. Another index of traffic performance is the speed of those bicycles influenced by pedestrians. As showed in Figures 11 and 12, yellow area represents higher speed performance than blue area. The result shows that bicycle speed is high at a low bicycle and pedestrian density level, which is intuitive because bicycle at free flow can travel with a high speed. It was found that bicycle speed decreased with the increasing bicycle and pedestrian density. The result is supported by previous researches [6, 7, 12]. An interesting finding is that bicycle

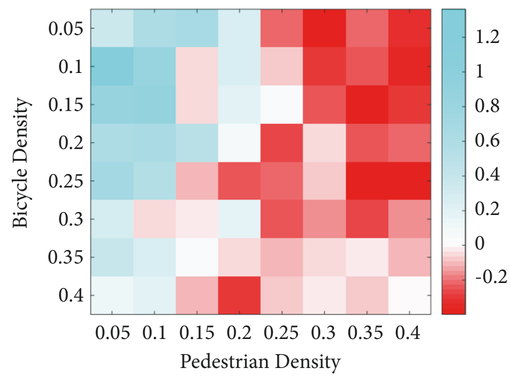

Figure 13: Difference of average influenced bicycle speeds between the scene with harbor-shaped bus stop and conventional bus stop.

speed at conventional bus stop area is higher than that at harbor-shaped bus stop area for the same bicycle and pedestrian density. The result confirms the impacts of harbor-shaped bus stop area on bicycle traffic flow, which can be also found in [8].

As shown in Figure 13, the average speeds of influenced bicycle at the two bus stops are similar under condition of higher bicycle density, regardless of the difference of pedestrian. However, when bicycle density reduces, conventional bus stop results in higher speed of bicycle travel when pedestrian density is low, while harbor-shaped bus stop has higher bicycle speed when the pedestrian density is higher.

5. Conclusions

In this study we assumed two different effects of bus stop along the bike path on bicycle traffic. The first effect is that some bus stop may occupy land space from bicycle path; another effect is the pedestrian number crossing the bicycle path to bus stops.

We set up cellular automation model to simulate these effects and calibrate the parameters' values considering the least sum square difference between simulated and empirical results.

Finally, we analysed the result of CA model. The increasing density of pedestrian crossing the street would reduce the bicycle speed and cause conflicts number to increase. On the other hand, conventional bus stop could provide wider range of positive performance condition in terms of both speed and conflict number comparing to the harbor-shaped bus stop, which limits the space for bicycle flow.

Nevertheless, the combination effect of bus stop types and pedestrian is much complex. When bicycle density is low, the effect of bus stop plays a little role in conflicts number but plays an important role in bicycle speed. Under this condition, conventional bus stop is preferred conditioning on low pedestrian density, while harbor-shaped is preferred conditioning on high pedestrian density. When bicycle density is high, there is limited effect of bus stop on bicycle speed, but not in conflicts number. Conventional bus stop is still preferred when pedestrian density is low and harbor-shaped bus stop performs better when pedestrian density is high.

Data Availability

The data used to support the findings of this study are available from the corresponding author upon request.

Conflicts of Interest

The authors declare that they have no conflicts of interest.

Acknowledgments

The work is sponsored by the Natural Science Foundation of Gansu Province (No. 1506RJZA109). And the research was conducted by the Bluesky studio at School of Transportation, Southeast University.

References

[1] J. Dales, P. Jones, R. Black et al., "International cycling infrastructure best practice study," in *Proceedings of the International cycling infrastructure best practice study*, 2014.

[2] Y. Guo, P. Liu, L. Bai, C. Xu, and J. Chen, "Red light running behavior of electric bicycles at signalized intersections in China," *Transportation Research Record*, vol. 2468, pp. 28–37, 2014.

[3] Y. Guo, Z. Li, Y. Wu, and C. Xu, "Exploring unobserved heterogeneity in bicyclists' red-light running behaviors at different crossing facilities," *Accident Analysis & Prevention*, vol. 115, pp. 118–127, 2018.

[4] Y. Guo, T. Sayed, and M. H. Zaki, "Evaluating the safety impacts of powered two wheelers on a shared roadway in China using automated video analysis," *Journal of Transportation Safety & Security*, pp. 1–16, 2018.

[5] Fitzpatrick, K., K. Hall, D. Perdinson, and L. Nowlin. TCRP Report 19: Guidelines for the Location and Design of Bus Stops. TRB, National Research Council, Washington, D.C., 1996.

[6] R. Z. Koshy and V. T. Arasan, "Influence of bus stops on flow characteristics of mixed traffic," *Journal of Transportation Engineering*, vol. 131, no. 8, pp. 640–643, 2005.

[7] J. L. Moura, B. Alonso, Á. Ibeas, and F. J. Ruisánchez, "A two-stage urban bus stop location model," *Networks and Spatial Economics*, vol. 12, no. 3, pp. 403–420, 2012.

[8] X.-M. Zhao, Z.-Y. Gao, and B. Jia, "The capacity drop caused by the combined effect of the intersection and the bus stop in a CA model," *Physica A: Statistical Mechanics and its Applications*, vol. 385, no. 2, pp. 645–658, 2007.

[9] X.-M. Zhao, Z.-Y. Gao, and K.-P. Li, "The capacity of two neighbour intersections considering the influence of the bus stop," *Physica A: Statistical Mechanics and its Applications*, vol. 387, no. 18, pp. 4649–4656, 2008.

[10] K. Fitzpatrick and R. L. Nowlin, "Effects of bus stop design on suburban arterial operations," *Transportation Research Record*, no. 1571, pp. 31–41, 1997.

[11] F. Zhang, Z. Li, and D. Zhao, "Influences of various types of bus stops on traffic operations of bicycles, vehicles and buses," *Transportation Research Board Annual Meeting*, 2015.

[12] Dehideniya Udugamage Ranasinge, Wathsala Jayanthi, Bunker, Jonathan M., & Bhaskar, Ashish (2017) Saturation headway variation at a signalised intersection approaches with a downstream bus stop and bicycle lane. In Australasian Transport Research Forum 2017, 27-29 November 2017, Auckland, New Zealand.

[13] M. Börjesson, C. M. Fung, S. Proost, and Z. Yan, “Do buses hinder cyclists or is it the other way around? Optimal bus fares, bus stops and cycling tolls,” *Transportation Research Part A: Policy and Practice*, vol. 111, pp. 326–346, 2018.

[14] H. Botma, “Method to determine level of service for bicycle paths and pedestrian-bicycle paths,” *Transportation Research Record*, no. 1502, pp. 38–44, 1995.

[15] Botma, H. Bicycle Planning in the Netherlands. Presented at the Helsinki University of Technology, April 1994. 7.

[16] Z. Li, W. X. Wang, J. Shan, J. Jin, C. Lu, and Yang., “Analysis of Bicycle Passing Events for LOS Evaluation on Physically Separated Bicycle Roadways in China,” in *Presented at 89th Annual Meeting of the Transportation*, Research Board, Washington, D.C, 2010.

[17] Z. Li, W. Wang, P. Liu, J. Bigham, and D. R. Ragland, “Modeling bicycle passing maneuvers on multilane separated bicycle paths,” *Journal of Transportation Engineering*, vol. 139, no. 1, pp. 57–64, 2013.

[18] C. Minh, K. Sano, and S. Matsumoto, “Characteristics of passing and paired riding maneuvers of motorcycle,” *Journal of the Eastern Asia Society for Transportation Studies*, vol. 6, pp. 186–197, 2005.

[19] H. Liu, H . Wang, and Y. H. Feng, “Bicycle flow modeling based on cellular automata,” in *Proceedings of the 2008 Chinese Control Conference (CCC)*, pp. 527–531, Kunming, China, July 2008.

[20] G. Gould and A. Karner, “Modeling bicycle facility operation: cellular automaton approach,” *Transportation Research Record*, no. 2140, pp. 157–164, 2009.

[21] D. Zhao, W. Wang, C. Y. Li, Z. B. Li, P. M. Fu, and X. J. Hu, “Modeling of passing events in mixed bicycle traffic with cellular automata,” *Transportation Research Record*, no. 2387, pp. 26–34, 2013.

[22] Y. J. Luo, B. Jia, J. Liu, W. H. K. Lam, X. G. Li, and Z. Y. Gao, “Modeling the interactions between car and bicycle in heterogeneous traffic,” *Journal of Advanced Transportation*, vol. 49, no. 1, pp. 29–47, 2015.

[23] S. Xue, B. Jia, R. Jiang, X. Li, and J. Shan, “An improved Burgers cellular automaton model for bicycle flow,” *Physica A: Statistical Mechanics and its Applications*, vol. 487, pp. 164–177, 2017.

[24] AASHTO (2001). A policy on geometric design of highways and streets, American Association of State Highway and Transportation Officials, Washington, D.C.